

# A New Short Pulse Diagnostics Line for Vulcan Petawatt

Contact [alexis.boyle@stfc.ac.uk](mailto:alexis.boyle@stfc.ac.uk)

A Boyle, M Galimberti, I Musgrave, S Spurdle

Central Laser Facility, STFC Rutherford Appleton Laboratory  
Chilton, Didcot, Oxon. OX11 0QX

## Introduction

Diagnostics on high power laser facilities are needed to qualify the performance of the system. Up to April 2012, the Vulcan PW beam line has relied on the full size beam diagnostics for both spatial and temporal characterisation measurements. The full size beam diagnostics take the leakage through the back of the mirror (M2) at the output of the compressor. Spatially, the full size diagnostics are a very powerful tool for near field (NF) characterization, due to the use of image relaying from the second grating. This also enables the diagnosis of damage to the optics in the compressor. However, the sampling method leads to undesirable nonlinear effects, as the beam passes through M2 and the diagnostics lens. The B-integral gives a good indication of whether a pulse will be affected by nonlinear effects. In the past, Self phase modulation (SPM) has been observed whilst trying to measure the spectrum on the full size diagnostics channel.

The new M2 diagnostics beam line reduces the pulse degradation effects by reducing the B-integral. This is achieved by sampling a small portion of the beam via a hole in M2. This beam line is then split into a high and low energy channels and sent to a diagnostics suite outside the compressor chamber. The arsenal of diagnostics on this table include: NF, far field (FF), spectrum, autocorrelation and Grenouille.

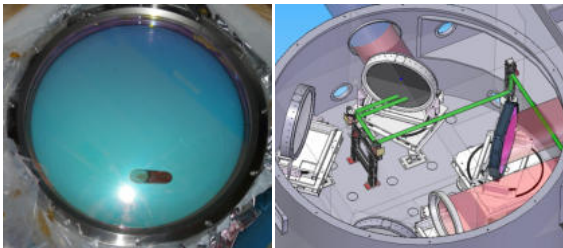


Figure 1: Photo of M2 mirror with 50 mm diameter hole drilled through at 45 degrees (left). 3D CAD model of the M2 diagnostic beam line.

## M2 Mirror

A 50 mm diameter hole was drilled at 45 degrees (figure 1 left). The hole was drilled near the bottom of M2 on the vertical centre line, 260 mm centre to centre. The spatial chirp across the NF is best sampled by the central hole location.

## B-Integral Calculations

The B-integral is calculated using equation 1<sup>[1]</sup>, where  $\lambda$  is the central wavelength of the pulse and  $n_2$  is the nonlinear refractive index of the propagation material. For the full size diagnostics channel, passing through the back of the M2 mirror and the large diagnostics lens is approximately 2. A general rule of thumb is to keep the B-integral less than 1.

Initially, the propagation out of the compressor chamber was designed to include relay imaging using two long focal length lenses. Calculations suggested that the B-integral was too high to achieve reliable short pulse measurements, so the lenses were removed from the design.

## Propagation Inside the Compressor Chamber

The propagation inside the compressor chamber can be seen in figure 2. M2 has two positions, 45 degrees (shown in fig 1 right) and in retro (fig 2 upper left) for compressor alignment. The sample beam passing through the hole is collected by a 3" silver mirror and propagates 5-6 m to the output flange of the compressor. The beam is reflected off four 4" silver mirrors attached to the compressor chamber. At the output, the beam is split into two using an uncoated glass plate and the remaining high energy by another 4" silver mirror. The high energy beam is approximately two orders of magnitude higher energy than the low energy beam. Three of the mirrors are fitted with drive motors to allow for remote alignment under vacuum. The 3" pick off mirror is also on a motorised slide to account for the two different positions of the sample hole in operational and retro alignment mode.

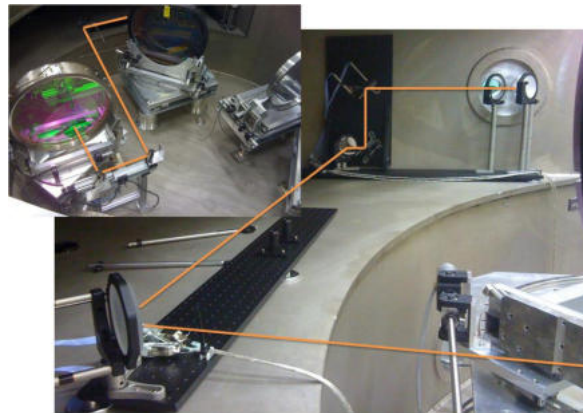


Figure 2: Pictures of TAP compressor chamber with overlay (orange) M2 diagnostic beam line.

## M2 Diagnostics Table

Due to space constraints on that side of the compressor chamber, the diagnostics breadboard had to be mounted vertically. A special breadboard was constructed with a letter box hole allowing the high and low energy beams to pass through. The initial design of the breadboard optics is shown in figure 3, along with a photo of the actual diagnostics setup. A periscope arrangement translates the beam on to the vertical table. The high energy line is split again using a 75:25 beam splitter to create a CW alignment channel and a high energy channel. All 3 beams then pass through 5:1 telescopes to reduce the beam size. The initial design shows the high and low energy lines passing through vacuum telescopes, however this is planned to be implemented at a later stage. For the time being, the 5:1 telescope is achieved with a positive negative lens setup,

this is to avoid focusing in the air. The CW line goes to NF and FF alignment cameras. The high and low energy lines are separated into various channels and are delivered to NF and FF cameras, spectrometer and several diagnostics bays. The diagnostics bays are back in the horizontal plane and accept standardised diagnostic setups built on 600 x 300 mm optical breadboards. These can be seen in figure 3 right. The standardisation of these diagnostics allow for plug and play installation in the bays. The beams are coupled to the bays by adjustable periscopes. In the current configuration, the M2 diagnostics house a NF autocorrelator<sup>[2]</sup> and a Grenouille.

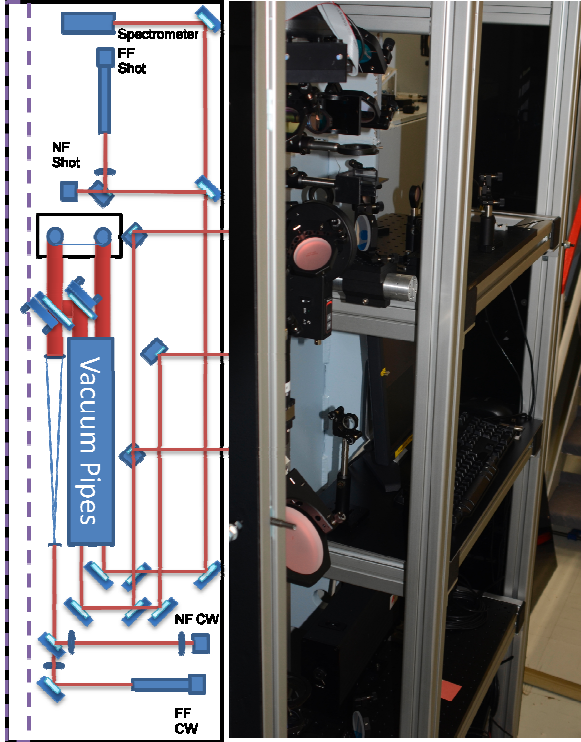


Figure 3: Initial design for the vertical breadboard (left). Photo of the current M2 diagnostics (right).

### Alignment

The alignment laser in LA4 does not produce a bright enough to propagate the hole and on to the optical table. During the alignment of the compressor, we implemented a pencil beam setup to boost the laser visibility whilst aligning the gratings. By moving this beam to match the hole position, the laser can be seen clearly on the M2 diagnostics. Sending the OPCPA bypass, it is also possible to align the autocorrelators in situ.

### Initial Results

Figure 4 shows the NF and FF traces from a full shot, >600J. We can clearly see fringes on the NF beam, caused by the beam passing through the hole in M2. The lack of image relaying on the beam line is worsening this effect. The fringe contrast is also high and we can see the effect of this on the NF autocorrelation and Grenouille traces in figure 5. The Grenouille trace is unusable as the retrieval software can not deal with this type of image. Despite the distinct fringes in the autocorrelation trace, a meaningful lineout is obtained and a pulse length of 570fs is measured. It is also the first time we have been able to measure the spectrum in TAP, without SPM effects, see figure 5.

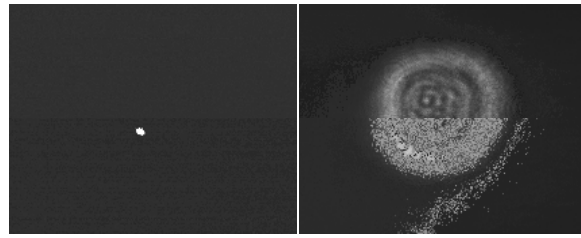


Figure 4: On shot FF (left) and NF (right).

The lack of image relaying on this diagnostics channel is clearly an issue, one that will not be easy to solve. A quick short term solution would be to replace the positive-negative telescopes to be positive-positive. This would involve introducing vacuum pipes to house the telescope arrangements, to avoid focusing in the air, see figure 3. This would provide some form of image relaying, even as far back as the M2 hole. The long term solution is to reintroduce the relay imaging inside the chamber. To reduce the B-integral, the majority of the energy would have to be dumped immediately after the hole. This would make alignment of the hole a bit of a challenge, if it were not for the pencil beam arrangement.

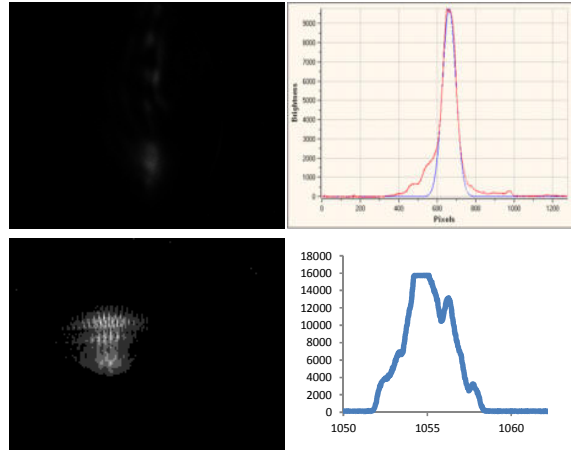


Figure 5: NF autocorrelation (top left), autocorrelation lineout (top right), enhanced Grenouille trace (bottom left) and saturated spectrum (bottom right).

### Conclusions

In this article we present the design and commissioning of the M2 diagnostics in TAP. Despite obvious problems in the NF quality due to not image relaying, the autocorrelator produces a reasonable results, 570fs. The spectrum is also good, if slightly saturated and does not exhibit any SPM. Improvement in the NF should improve the Grenouille trace.

### References

1. A. E. Siegman, Lasers
2. CLF Annual Report 2011-12, NF Autocorrelator

# Near Field Autocorrelator for High Power Lasers

Contact [alexis.boyle@stfc.ac.uk](mailto:alexis.boyle@stfc.ac.uk)

Alexis Boyle, Marco Galimerti

Central Laser Facility, STFC Rutherford Appleton Laboratory  
Chilton, Didcot, Oxon. OX11 0QX

## Introduction

It is now the general consensus amongst some European high power laser facilities that short pulse diagnostics are unreliable [1]. In general, post compression, short pulse diagnostics suffer from high B-integral, spectral dispersion, near field (NF) inhomogeneity and pointing stability. These issues can lead to inaccurate or nonsense pulse length measurements. For many years, Vulcan has used uniaxial autocorrelators (AC)[2], which use cylindrical lenses to boost the intensity on the crystal and the addition of pulse front tilt to increase the temporal window of the device. These, like most pulse characterisation devices work perfectly with the front-end oscillators, but fail to provide reliable measurements on shot in the target areas. Multiple autocorrelations have also been observed on one device, which causes ambiguity as to what trace to measure. It was decided to follow a simple approach to the problem, a purely NF AC.

## Design

All our NF ACs are based on the design show in figure 1. There are slight variations between the versions. The version shown in figure 1 has imaging of both IR beams, the TAW beam 7 AC show in figure 3 only images the green from the crystal.

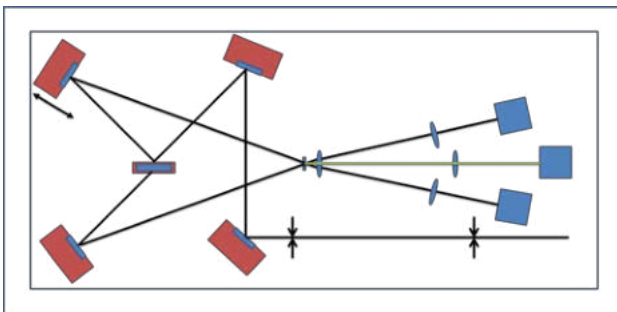


Figure 1: Schematic of NF AC design incorporating imaging of both the green autocorrelation and the two IR beams.

The two IR arms cross in the crystal near 45 degrees, the reason for this is twofold, to increase the temporal window of the device and allow space to fit two imaging lines for the IR arms, see figure 1. The first lens is placed as close as possible, ~10 mm, to the BBO crystal. This allows the two IR beams and the autocorrelation to be collected. All three lines image the plane at the input to the BBO crystal. All the lenses in the imaging use doublets to improve the imaging.

All the ACs are standardised, built on 600 x 300 mm breadboards with a common input height and position. This allows the AC to be calibrated in the front-end and dropped into place with minimal alignment issues. An adjustable periscope drops the beam to 50 mm off the breadboard for increased stability.

## Temporal Window

The temporal window is related to this angle and the crystal size. The limiting factor for the arm overlap angle is the phase matching condition in the BBO crystal. The limit is about 45 degrees. The crystal aperture is 6 mm diameter. The phase matching angle for BBO crystal is about 40 degrees, so we are using a crystal cut for 3<sup>rd</sup> harmonic Ti:Sapphire. Using the

temporal calibration plot we have a window of 7 ps from edge to edge, this is reduced to about 4 ps (factor of 1.5) for the full autocorrelation trace. We are confident the measurement is reliable over 2.5 ps window.

## Results

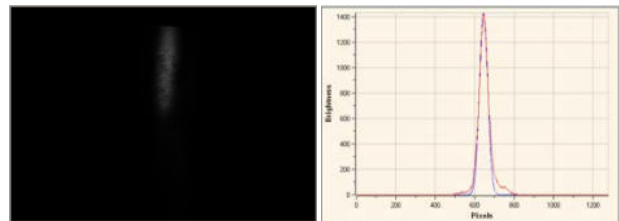


Figure 2: NF Autocorrelation trace captured from a 540J shot into TAP. FWHM corresponds to 600 fs pulse duration.

Figure 2 shows an example autocorrelation for a full disk shot in TAP, 540 J. The lineout of the trace suggests a pulse length of 600 fs. This is well within the temporal window of the AC and a believable result.

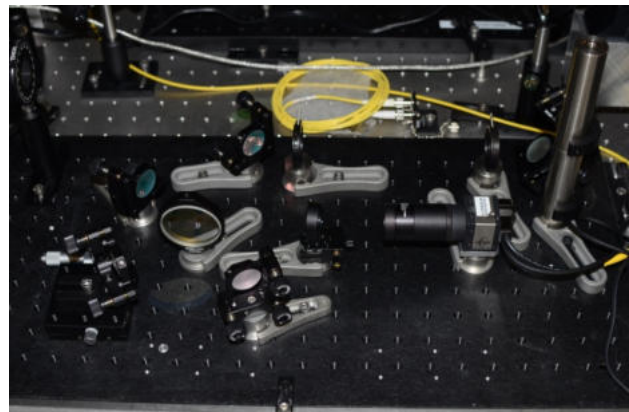


Figure 3: NF AC in TAW beam 7.

## Conclusions

Here we present a simplified NF autocorrelator design for full energy shot diagnosis. Preliminary results show autocorrelation traces in TAP of approximately 600 fs. The NF devices seem more stable than the uniaxial ACs, providing a measureable trace on nearly every shot. A completed NF AC that images the IR arms, shown in figure 1, will follow shortly. Further work is needed to increase the temporal window to greater than 10 ps using an image relayed grating to add pulse front tilt.

## References

1. NAHEL June 2012
2. Uniaxial Single Shot Autocorrelator. Review of Scientific Instruments, Vol 70, No.3. 1999.

# Mixed glass rod chain optimisation

Contact [marco.galimberti@stfc.ac.uk](mailto:marco.galimberti@stfc.ac.uk)

M. Galimberti, A. Boyle, I. Musgrave, B. Parry, T. Winstone

Central Laser Facility, Science and Technology Facilities Council  
Rutherford Appleton Laboratory, Harwell Science and Innovation Campus, Didcot, OX11 0QX

## Introduction

To enhance the final bandwidth of the pulse in the beamline for the Target Area Petawatt, a mixed glass rod chain was in use, adding to the standard Nd:phosphate amplifiers some Nd:silicate amplifiers. Because the Nd:silicate has the amplification centered around 1060 nm, compared to the 1053nm of the Nd:phosphate, the mix allowed to obtain wider bandwidth. A study was performed to find the right balance between the two types of amplifiers [1]. However, after some years of operational, the balance changed, shifting the spectrum of the pulse in the red region, reducing drastically the gain into the disk amplifiers and affecting the final bandwidth and, as a consequence, the pulse duration and the peak power.

## Silicate rod chain characterization and new layout

In the previous configuration, the silicate chain was replacing one of the Nd:phosphate rod amplifier with two Nd:silicate rod amplifiers.

The beam from the diffraction limited pinhole (fig. 1a) was redirected by a cube polarizer to the first silicate amplifier, using a rod of 9mm (9B), after been collimated by a single lens. Successively a vacuum spatial filter (VSF) was used to increase the beam size before sent the pulse to a double pass Nd:silicate 16mm rod amplifier. Finally, the beam was re-injected into the phosphate rod chain bypassing the Nd:phosphate 16mm rod amplifier (16B). The VSF was detuned to match the divergence of the beam during a shot.

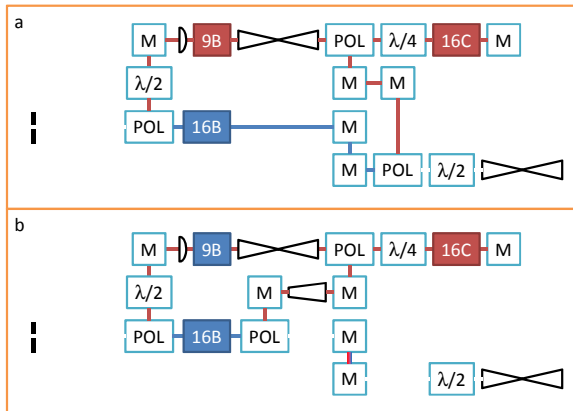


Fig. 1: Schematic of the silicate chain: a – old amplifiers configuration; b – new amplifiers configuration.

In order to characterize the amplifiers, a series of rod shots were taken with different amplifier configurations, using the OPCPA as a seed. The spectra were acquired at the corner, at the end of the rod chain. Taking into account the seed spectrum and the actual amplifier configuration, an estimation of the spectral gain for each amplifier was calculated, shown in fig. 2. For estimate the spectral gain of the disk amplifiers, a previous disk shot in TAP were used, comparing the spectrum in LA4 (i.e. at the end of the laser chain) with the spectrum at the corner.

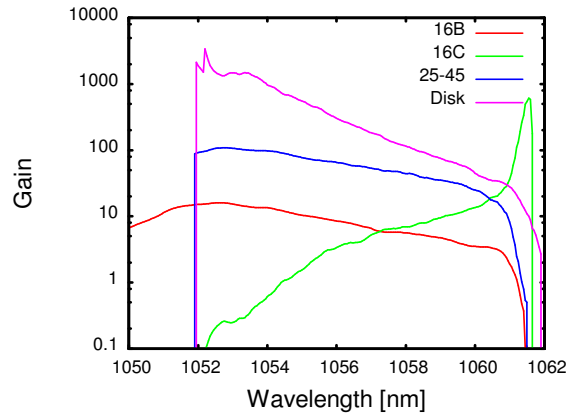


Fig. 2: Measured spectral gain for each amplifier.

While the spectral gains obtained show anomalies for wavelengths outside the interval 1053.5 nm – 1060 nm, there were still useful to calculate a better balance between silicate and phosphate amplifiers.

As a result it was clear that the actual configuration was any more not optimal: to obtain a balanced amplification spectrum the 9B amplifier was not required. However, without that amplifier, the overall gain was not enough to provide the required energy so another amplifier was still required.

In order to address the issue, the silicate chain was modified as shown in fig. 1b. The initial part was left the same as before, up to the 9B. The 9B rod was replaced with a phosphate rod: the phosphate has a spectral gain more balanced compared to the silicate over the required spectral region.

The VSF was modified to be able to provide a parallel beam at the output. After the same silicate amplifier (16C) in the same double pass configuration, the beam was conditioned by a positive-negative beam expander to modify the beam size and the divergence before to be re-inject into the phosphate chain.

Compared to the previous setup, the beam into the 16C amplifier is now collimated: in this way the beam divergence is less affected to the changing of the refractive index when the rod is pumped.

The injection was moved earlier to be able to use the diagnostics for the 16B to monitor the output of the silicate chain.

## Results

After changed the setup, a series of tests were performed to characterize the new silicate chain. In particular, the change of the 9B from silicate to phosphate required a tuning of the flash lamp voltage, in order to provide the required energy but without reducing the final bandwidth.

The final balance was able to provide the spectra in fig. 3. The spectrum of the pulse from the OPCPA was quite uniform across the bandwidth. After the rod chain, in green, the spectrum was modified with a triangular-type shape with more intensity in the red region.

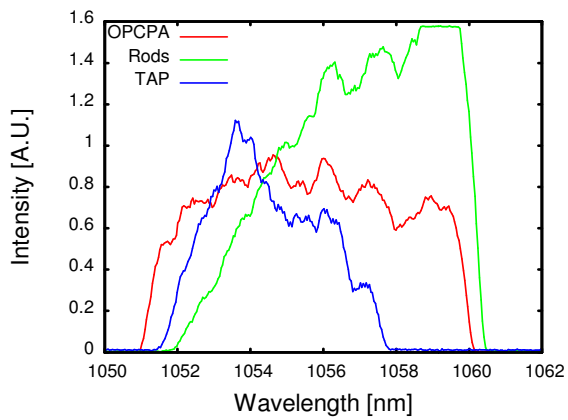


**Fig. 3: Spectra acquired during a full power shot in TAP.**

At the end of the chain, in blue, the bandwidth is reduced to around 4.5nm around 1054.5nm. This bandwidth is capable to provide pulses of 365 fs, considering a Gaussian spectral shape.

### Focal spot

In the previous configuration the VSF into the silicate chain was detuned to compensate a change in divergence of the beam during the firing of the amplifiers, previously observed in the silicate chain only.

Because the optical system was changed, a new investigation was required. To do so, a series of low power shots were performed, looking the far field at the end of the laser chain, in LA4.

The results are shown in fig. 4. The far field obtained with the phosphate chain is well in agreement with the one obtained with the silicate, without the requirement of the detuning of the VSF.

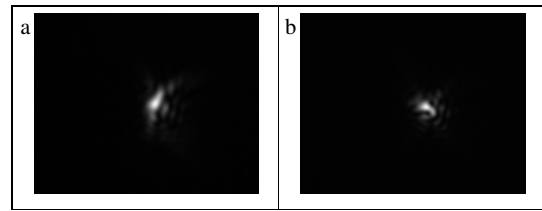


**Fig. 4: Focal spot in LA4 on a low power shot: a – phosphate chain; b – silicate chain.**

### Conclusions

After some years of operations of the Vulcan in TAP, an unbalance between the silicate and the phosphate amplifiers were observed and degraded the performance of the Vulcan.

A series of tests were performed and the silicate chain was redesigned to re-optimize the final bandwidth of the pulse.

Within the new layout a 4.5nm bandwidth was measured during a full power shot in TAP.

The new configuration shows also less influence into the divergence of the beam during a shot.

### References

- [1] S. Hawkes et al., “Mixed glass rod amplifier chain – design and implementation”, pag. 169, CLF Annual Report 2003/2004
- [2] S. Hawkes et al., “Pump induced aberration characterization and compensation for the Vulcan Petawatt beam”, pag. 194, CLF Annual Report 2004/2005

# Vulcan Target Area West Commissioning

Contact [margaret.notley@stfc.ac.uk](mailto:margaret.notley@stfc.ac.uk)

M. M. Notley, A. Boyle, A. Cox, R. J. Clarke, O. Ettliger, A. Frackiewicz, M. Galimberti, R. Heathcote, D. Johnson, K. L. Lancaster, I. Musgrave, D. Rusby, J. Suarez-Merchan, T. B. Winstone

Central Laser Facility, STFC, Rutherford Appleton Laboratory, Didcot OX11 0QX

## Introduction

Target Area West has dual CPA short pulse facilities specified to deliver 1ps, 100J (beam 7) and a range of 1-10ps in up to 100 - 300J respectively (beam 8). The operations team has recently conducted a commissioning project to characterise, quantify and benchmark its capabilities. Presented here are the results of the campaign to measure beam quality, focal spot size and pulse length of the system, improving them where possible and necessary. These characteristics were also tested in combination via interaction of laser pulses on target. This gives knowledge about the intensity deliverable inferred from output peak proton signal and dosimetry measurements.

These aspects define the ability of this facility to deliver high intensity ( $>10^{18}\text{W}/\text{cm}^2$ ) to target and have been pinpointed as desirable characteristics to quantify, benchmark and communicate to our research community.

## Beam quality and Focus

The ability to focus is of fundamental importance (along with pulse length) when aiming for high intensity interactions. The TAW facility had seen a decline in the ability to obtain a small focal spot and a programme of investigation was carried out. A diagnostic test was set-up and conducted after every accessible optic in the system. The ability to focus the beam at each point was measured, the aberrations present identified and if there were significant issues a fix was implemented where this was possible.

The tests were carried out using a long focal length lens (3.65m) to focus the beam and a 12 bit ccd with a x10 objective lens to image the focus. With the beam being 200mm square or circular, the F/# of this system, and diffraction limited spot size is  $\sim 18.375\mu\text{m}$  FWHM.

An example of our investigation is shown in figs 1a & 1b. Images of the beam coming off on an optic before and after correction to the mount.

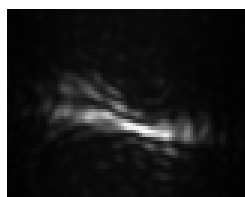


**Figure 1a** image of focus showing aberrated spot  $\sim 120\mu\text{m}$  long,  $25\mu\text{m}$  wide



**Figure 1b** image of focus corrected. Spot is  $23\mu\text{m}$  FWHM, 1.25x diffraction limited

Investigation identified that a number of the optical mounts had over time become tightened leading to some severe astigmatic

D. Carroll, M. Coury.

University of Strathclyde, OX11 0QX, UK

aberrations like that shown in Fig 1a. All the accessible mounts have been adjusted to prevent this occurring in future.

Once optics prior to the interaction chamber had been investigated and adjusted the parabolaes were installed into both beams and optimized to check best obtainable focus. A comparison between the CW 1053nm beam and the 9 second cycle (which delivers bandwidth) was carried out. Differences that might be observed between single and multiple wavelengths here can lead to identification of pulse compression system issues.

For high intensity experiments TAW CPA beamlines are focused to target currently using F/3 parabolic mirrors. Typically one would expect, with a diffraction limited beam, to be able to obtain a focus of around 3-4 microns FWHM.

With the improvements made to the system the facility is able to deliver  $4.5 \times 6\mu\text{m}$  spot on beam 7 and  $6 \times 8\mu\text{m}$  spot on beam 8. These are 1.5 and 2.5 diffraction limited respectively. So there is still room for improvement, but this result is a huge improvement on the situation previously, as shown in figures 2a, 2b which compare Beam 7 results.

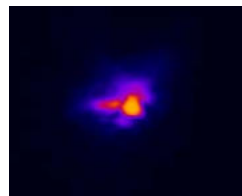


**Figure 2a**  
Foci B7 March 2011, CW spot above, 9 sec cycle spot below

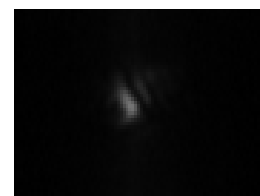
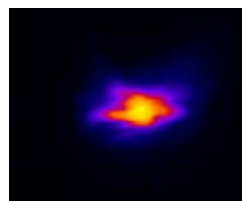


**Figure 2b**  
Foci B7 August 2011, CW spot above, 9 sec cycle spot below

18.5 x 10  $\mu\text{m}$  focus CW,  
27.3 x 15  $\mu\text{m}$  focus 9 sec  
6x diffraction limited  
Possible spectral dispersion

4.5 x 4.6  $\mu\text{m}$  both CW & 9sec cycle  
1.5x diffraction limited

## Pulse compression

Pulse length is the second highly influential characteristic that has an impact on the intensity achievable. Through this campaign the alignment of the TAW stretcher, compressor and diagnostics for measuring the pulse length have all been

checked and where necessary adjusted and calibrated. Along the way some important realisations have come to light about how single pass compressor systems are exceedingly sensitive to the input collimation of the beamline. The collimation has therefore also been checked and set on both the internal and external beamlines that are used in TAW and also in TAP. A new technique has since been introduced for re-commissioning when adjustments to any of our single pass systems need to be made.

Overall TAW is specified to deliver pulses on beams 7 & 8 at 1ps or 10ps. Beam 7 is usually set to 1ps and beam 8 varied between 1 and 10ps dependent on experiment requirements. For this project beam 7 was set to be optimized at its shortest pulse length and beam 8 to nominally 10ps.

Auto-correlators that are used to measure on shot pulse length that are permanently located (after an optic in the compressor) were compared to pulse length measured directly at target. The pulse length measurement tests revealed that TAW can achieve a 1ps short pulse as specified (see fig 3). The longer pulse was measured using a Hamamatsu C5680 streak camera with a best resolution of 8ps. The pulse length of beam 8 is variable but in this case measured to be 12ps.

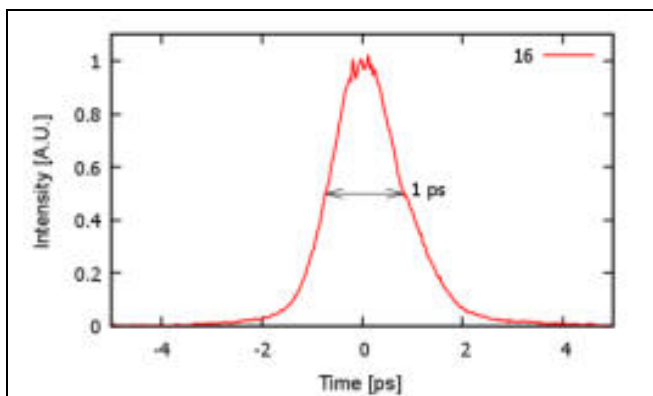


**Figure 3** Line out of beam 7 autocorrelation showing 1ps FWHM

### Intensity delivered

There are many physical processes in experimental campaigns undertaken on Vulcan Facilities that require a high intensity of a laser pulse to work. The ways in which pulse length, energy, and intensity all together intermingle to give an end result are complex. There are however some indicators which one can use to infer that the intensity is above certain levels.

To benchmark the TAW dual CPA, shots to target were carried out to obtain data on peak proton energy production and x-ray dose – both of which are intensity dependent processes.

To perform these tests gold foils of 10 & 20 micron thickness were employed to produce protons, diagnosed by a film pack containing radiochromic film (HD810 combined with mylar).

Figures 4 & 5 show the resultant proton beam – the peak energy, proton beam profile and the depth of colour gives an indication of total flux which can be further analysed to give a dose measurement. The film stack recipe employed uses 50mm square RCF HD810 films with 300µm mylar in between from sheets 2 – 10, then 600µm mylar in between RCF sheets from there onward up to 20 layers. The whole pack was wrapped in Al foil 13µm thick. The pack was placed 5 cm from target. The range of detectable proton energies with this pack goes from 1.2 to 38 MeV

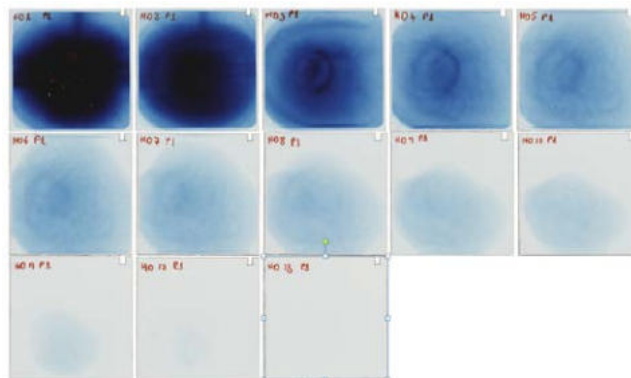


**Figure 4** 10µm gold foil, 95J, 1ps on Beam 7. 25MeV proton peak energy measured with RCF HD810

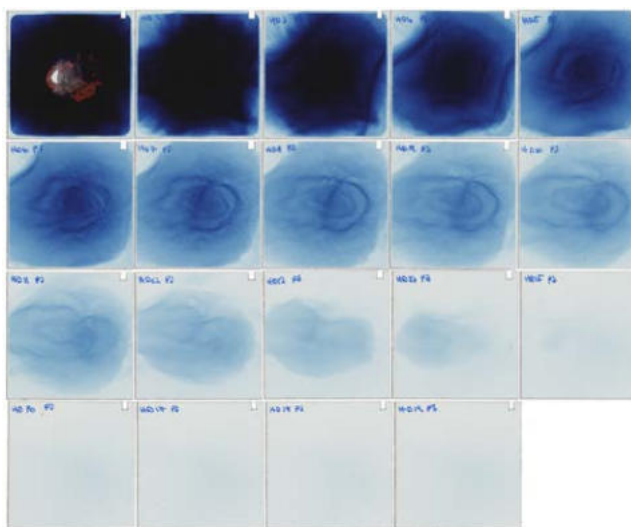


**Figure 5** 10µm gold foil, 240J, 12ps on Beam 8, 28Mev proton peak energy measured with RCF HD810. A further shot with 300J and a 20µm foil was also taken resulting in 35MeV peak result.

X-ray dose was characterised using 3mm thick tantalum targets, diagnosed with TLD arrays. The dosimetry results as a function of linear density (filtering) of the TLD stack match well with data taken at similar intensities in the Petawatt Target Area at similar intensities, producing well over an order of magnitude increase in dose over data prior to the system corrections described through this report.

### Conclusions

The TAW facility has now been commissioned and shown to perform to specification 1ps, 100J, or 10ps, 300J. Focus of 1.5 and 2.5 x diffraction limit. The system can deliver intensities high enough to produce proton cut off energy of 25MeV( Beam 7) and 35MeV (Beam 8). For this to occur the intensity should be in the region of  $>10^{18} \text{ Wcm}^{-2}$  which is what we would expect from the specifications that TAW was designed to meet.

There is room for further improvement and there are plans to enhance the system in the future.

### Acknowledgements

Many thanks to the team of staff who have made this possible.

# Refurbishment of Vulcan Target Area Petawatt

Contact [trevor.winstone@stfc.ac.uk](mailto:trevor.winstone@stfc.ac.uk)

TB Winstone, A Boyle, RJ Clarke, AJ Frackiewicz, M Galimberti, J Green, R Heathcote, IO Musgrave, MM Notley, C Hernandez-Gomez

Central Laser Facility, STFC Rutherford Appleton Laboratory  
Chilton, Didcot, Oxon. OX11 0QX

## Introduction

Since commissioning the Vulcan 1 PW Facility [1] in 2002 it has delivered 2493 high energy shots to target. Following degradation of the near field a decision was made to run at a lower intensity on the large aperture optics to extend their operational lifetime. Between April and August 2011 the large aperture optics were replaced and the system recommissioned.

## Inspection: April 2009

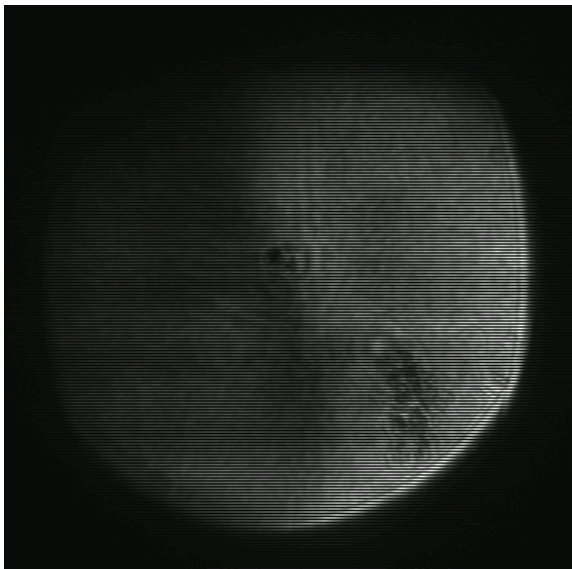


Figure 1: Near field of the Vulcan Petawatt Facility in April 2009.

In April 2009 the previously clean near field of the beam being delivered to Target Area Petawatt (TAP) started to degrade, showing signs of an 'S' shaped shadow across one half of the

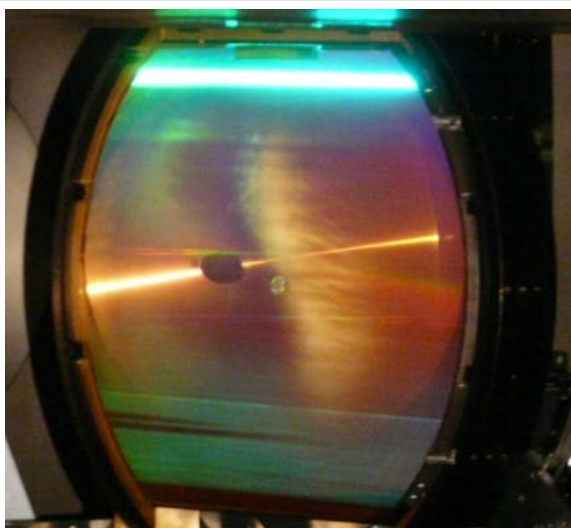


Figure 2: North gold compression grating as viewed from the South compressor tank. Clearly visible is the 'S' shaped burn in the gold grating surface.

beam coupled with a speckled section.

At the next available opportunity the compressor was let up and the optics inspected. The cause of the 'S' shaped shadow was quickly found when the second gold grating (North) was found to be suffering from a generalised laser damage area (see figure 2) in the shape of an 'S' which perfectly matched the shadow shaping in the near field image.

Further inspection revealed a 'delamination' of the final mirror

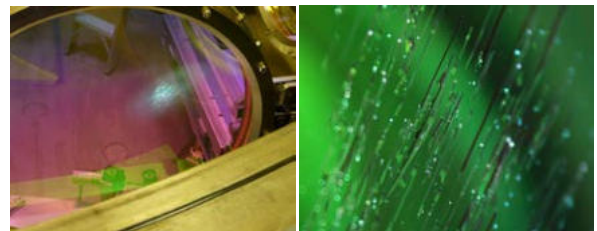


Figure 3: Final turning mirror in compressor a) View as lids are removed showing patch of delamination b) close up showing coating layers lifting from optic surface

before the interaction chamber.

It was already known that the final focussing parabola was suffering from a level of coating damage, where the protective overcoat was damaged leaving the silver surface exposed across one half of the beam. This unprotected side had, over time, become oxidised, further reducing the reflectivity of the optic.

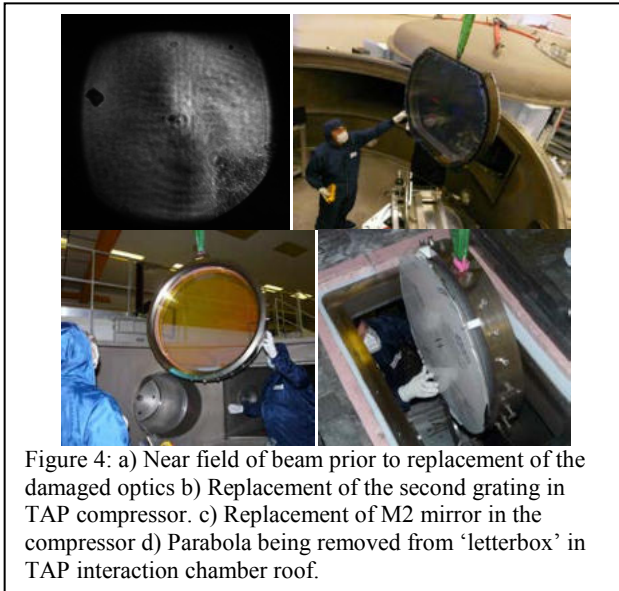
As an operational facility it would not be possible to schedule access to the compressor for an extended period until April 2011. The deliverable energy level from the laser was reduced from 600 J to 300 J to ensure the survival of the damaged optics until the refurbishment period.



Figure 4: Damage across half the beam area of the protective overcoat on the silver coated final focusing parabola

## Replacement of large aperture optics

Over this period the near field diagnostics showed a continual gradual degradation of the beam both in the area of the 'S' shaped burn on the grating and the speckle caused by the 'delamination' of mirror M2.



During a 3 week period in April 2011 the large aperture optics were replaced. To best maintain the alignment of the compressor, and so reduce the turnaround timescale, the project would see the replacement of one grating and the realignment of the new grating with the other old grating. However after replacing the first grating it was not possible to produce a single spot in the far field whilst using 2 laser wavelengths (1047 nm and 1053 nm), but only two distinctly separated spots. The data was analyzed and the conclusion drawn that the two gratings had a slightly different line density. This mismatch in the line density was verified by measurement and found that the original gratings had a line density of 1480 lines/mm, whereas the replacement gratings had a line density of 1490 lines/mm. This may be possible through the manufacturing process as the two grating pairs are exactly matched to each other, having been manufactured during consecutive exposures. However there is no guarantee that different sets of gratings manufactured several years apart will exactly match. The only way to fully verify this was to replace the other grating. Once replaced the new pair of gratings could be aligned parallel and produced a single spot at two wavelengths in the far field. Following the replacement of M2 the whole system was realigned.

**Additional diagnostics line**

The diagnostics for the Vulcan Petawatt beamline have always been taken through the back of the M2 mirror. However this has led to issues with the near field and far field diagnostics such as the autocorrelator for measuring the compressed pulse length. This has been modeled and it is believed that the far field is largely influenced by the Breakdown integral or B-integral[2] which is extremely large for short pulse beams travelling through air and glass. As the M2 mirror transmits about 2% of the incident energy (of the order of 10 J) in a nominally 500 fs pulse through a 100 mm thick BK-7 glass this will give a large B-integral, of the order of 4, which is significant for a femtosecond pulse. To attempt to get around

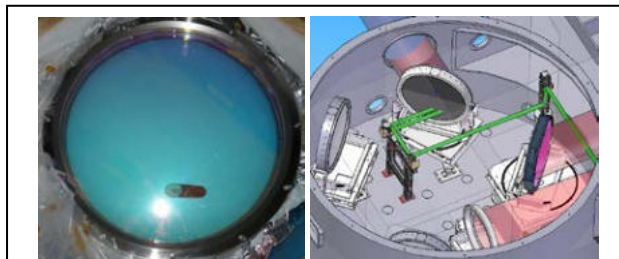
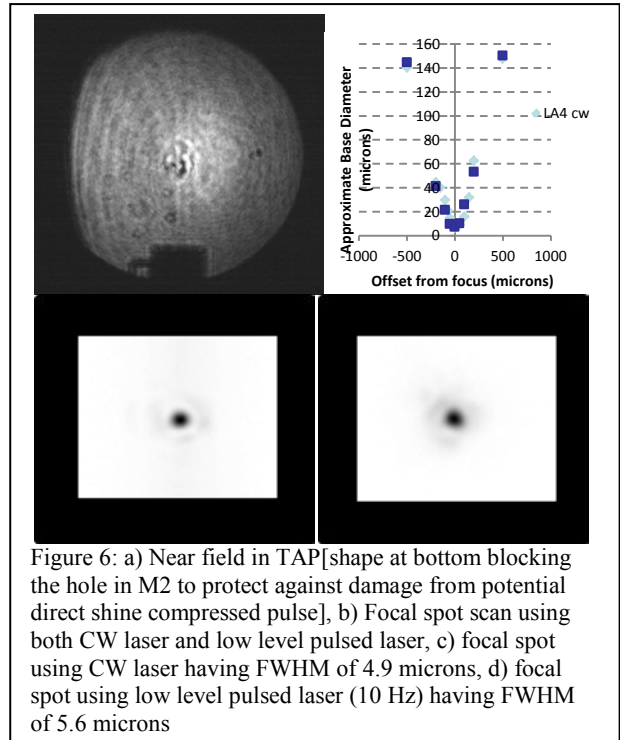


Figure 5 a) New M2 mirror with 50 mm dia hole drilled through it at 45 degrees b) Schematic of the beamline through the M2 hole for the diagnosis of the beam with reduced B-integral

this issue a hole has been drilled through the M2 mirror during the reworking process prior to coating, and a beamline designed and installed to take the M2 beamlet outside of the compressor chamber to a suite of diagnostics[3]. This should enable diagnosis of the short pulse without the B-integral effects.

**Recommissioning TAP**



After such a major intervention in to the alignment and operation of the Vulcan Petawatt Facility it was essential to

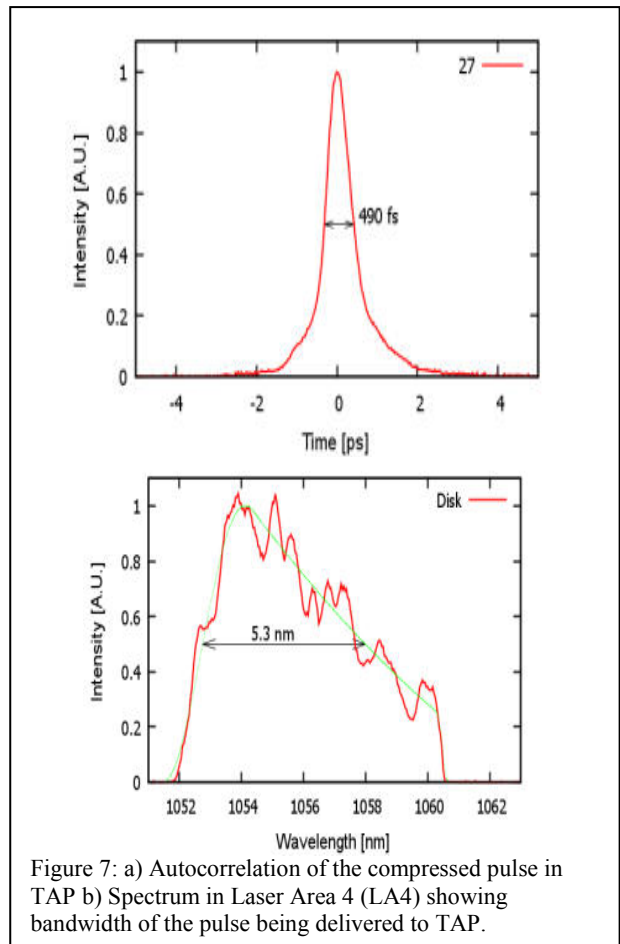


Figure 7: a) Autocorrelation of the compressed pulse in TAP b) Spectrum in Laser Area 4 (LA4) showing bandwidth of the pulse being delivered to TAP.

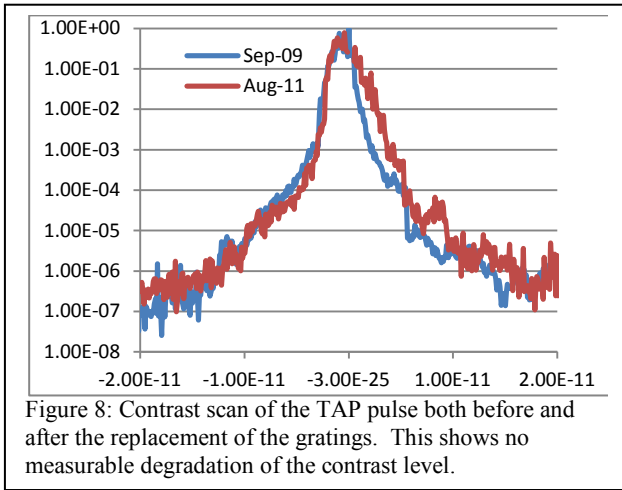


Figure 8: Contrast scan of the TAP pulse both before and after the replacement of the gratings. This shows no measurable degradation of the contrast level.

prove that the facility was operating at a sensible level. A plan was drawn up to check the Near field, far field (figure 6), pulse length, spectrum (figure 7), contrast levels (figure 8), and the ability to produce protons (figure 10).

The characterisation of laser-driven proton beams provides valuable information on the performance of several aspects of the laser including: energy on target, peak intensity, focal spot uniformity and contrast. In order to qualitatively assess these key performance parameters a number of full power shots were taken in the Vulcan Petawatt target area. 20 µm Au foils were irradiated at intensities of up to  $10^{21}$  Wcm<sup>-2</sup>. A Radiochromic Film Stack (RCF) was placed 50 mm behind the target in order to characterise the proton beam spatial and spectral distribution.

A laser energy scan was performed, with the maximum proton energy determined for each shot (see Figure 9). The highest proton energy (45 MeV) was seen for the maximum on-target energy of 382 J. It is interesting to note that the peak proton energy appears to plateau for laser energies at least 100 J below this figure.

The proton beam profiles exhibited circular symmetry (see Figure 10) for all but the highest proton energies. Together with the observed peak proton energy of 45 MeV, this seems to confirm a good focal spot profile as seen in Figure 6. The thinnest target shot during the data scan was 5 µm, for which similar proton energies were seen as in Figure 9. Unfortunately thinner targets were not available during the data run, so the lower limit of target thickness that could successfully generate protons without any negative effects of pre-pulse disruption could not be determined.

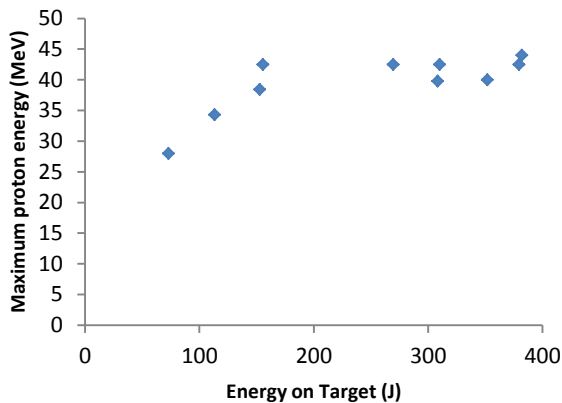


Figure 8: Maximum proton energy as a function of laser energy on target for 20 µm Au foils.

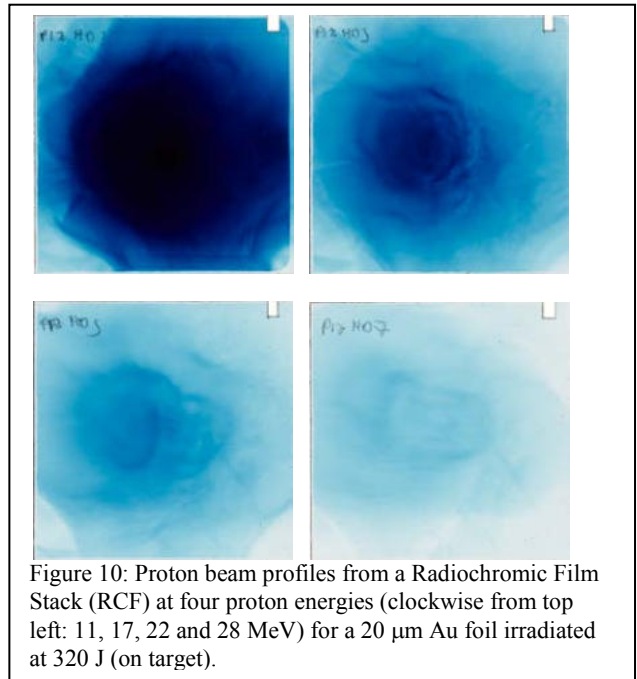


Figure 10: Proton beam profiles from a Radiochromic Film Stack (RCF) at four proton energies (clockwise from top left: 11, 17, 22 and 28 MeV) for a 20 µm Au foil irradiated at 320 J (on target).

### Conclusions

The damaged large aperture optics within the compressor and target chamber have been replaced. This has led to a significantly improved near field of the TAP short pulse beamline enabling operation at 600 J from laser. Following a commissioning period we have characterised the Petawatt Facility and delivered protons at the 45 MeV level from a 10 micron Gold foil.

Vulcan 1 PW Facility is now operational and has delivered an experiment at higher energies.

### References

1. Vulcan Petawatt – Compressor and system commissioning, JL Collier et al, CLF Annual Report 2002-03
2. High Peak power Nd:glass laser systems, DC Brown, Springer series in Optical Sciences, ISBN 3-540-10516-6
3. A Boyle, CLF Annual Report 2012